Case Studies in Thermal Engineering 39 (2022) 102430

Contents lists available at ScienceDirect

Case Studies in Thermal Engineering

journal homepage: www.elsevier.com/locate/csite

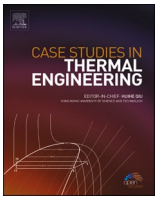

Experimental investigation of the influence of ethanol and biodiesel on common rail direct injection diesel Engine's combustion and emission characteristics

Phyo Wai [a], Phobkrit Kanokkhanarat [a], Ban-Seok Oh [a], Veerayut Wongpattharaworakul [a], Nattawoot Depaiwa [a], Watcharin Po-ngaen [b], Nuwong Chollacoop [c], Chadchai Srisurangkul [d], Hidenori Kosaka [e], Masaki Yamakita [e], Chinda Charoenphonphanich [a], Preechar Karin [a,*]

[a] School of Engineering, King Mongkut's Institute of Technology Ladkrabang, Bangkok, 10520, Thailand
[b] Faculty of Technical Education, King Mongkut's University of Technology North Bangkok, Bangkok, 10800, Thailand
[c] National Energy Technology Center, National Science and Technology Development Agency, Pathum Thani, 12120, Thailand
[d] National Metal and Materials Technology Center, National Science and Technology Development Agency, Pathum Thani, 12120, Thailand
[e] School of Engineering, Tokyo Institute of Technology, Tokyo, 152-8552, Japan

ARTICLE INFO

Keywords:
Biodiesel
Ethanol
Diesel engine
Combustion characteristics
Particle emission

ABSTRACT

This study aims to characterize the effect of oxygenated biofuels in diesel engine combustion, thermal efficiency, and emission by blending different percentages of ethanol and biodiesel with fossil fuel derived diesel. In this research, 5% and 10% by weight of bioethanol were added to commercial B10 (10% biodiesel and 90% diesel), B20 (20% biodiesel and 80% diesel) and B100 (100% biodiesel) and experimented on using a 3 L four-cylinder common rail diesel engine. The experiment was performed under three engine speeds of 1000 rpm, 1500 rpm, and 2000 rpm with three constant engine torques of 56 Nm, 84 Nm, and 140 Nm. The results show that ethanol-biodiesel-diesel ternary blended fuels are higher in premixed combustion pressure and net heat release rate (NHRR) peaks. The cumulative heat release of ethanol blended fuels is also higher for ethanol blended fuels. The fuel consumption increased with the ethanol and biodiesel percentage in the blended fuels due to the lower heating value while the brake thermal efficiency did not decrease. It was clearly observed that the particle emission could be reduced by more than 50% when ethanol and biodiesel percentage increased.

* Corresponding author.
E-mail address: preechar.ka@kmitl.ac.th (P. Karin).

https://doi.org/10.1016/j.csite.2022.102430
Received 11 July 2022; Received in revised form 14 August 2022; Accepted 14 September 2022
Available online 15 September 2022

Nomenclature

B10	10% biodiesel and 90% diesel blended fuel
B20	20% biodiesel and 80% diesel blended fuel
B100	Pure biodiesel
B10E5	5% ethanol and 95% B10 blended fuel
B10E10	10% ethanol and 90% B10 blended fuel
B20E5	5% ethanol and 95% B20 blended fuel
B20E10	10% ethanol and 90% B20 blended fuel
B100E5	5% ethanol and 95% biodiesel blended fuel
B100E10	10% ethanol and 90% biodiesel blended fuel
ECU	Engine control unit
EGR	Exhaust gas recirculation
OBD	On board diagnosis tool
MPRR	Maximum pressure rise rate
NHRR	Net heat release rate
CNHR	Cumulative net heat release
BSFC	Brake specific fuel consumption
BTE	Brake thermal efficiency
NO_x	Nitrogen oxide
CO_2	Carbon dioxide
THC	Total hydrocarbon
PM	Particle mass

1. Introduction

Internal combustion engines are generally used for human activities such as transportation, communication, and industry. The internal combustion engine that remains the main power source for transportation, agriculture, and heavy industry application is the compression ignition diesel engine. The diesel engine has a high compression ratio with respect to high torque and high thermal efficiency. Due to the above reasons, the demand for diesel vehicles remains considerable. As the demand for diesel vehicles has grown, diesel consumption has also increased and has greatly contributed to fossil fuel shortages. In addition, a significant disadvantage of diesel engines is the emission of nitrogen oxides and smoke. The emissions from combustion engines are carbon monoxide (CO), nitrogen oxides (NOx), hydrocarbons (HCs), and particulate matter (PMs), which mostly come from incomplete combustion [1][R. Zhu, C.S. Cheung, Z. Huang, X. Wang]. Intensified pollution control regulations have led to many researchers investigating numerous strategies to minimize the emissions, such as advanced combustion techniques, exhaust after-treatment systems, and using alternative fuels derived from renewable sources like biodiesel [2] [P. Verma.et al.].

V. H. Nguyen et al. [3] investigated biodiesel from residues taken from a palm cooking oil manufacturing process in different biodiesel-diesel blends and compared it to the fossil diesel on a cooperative fuel research engine under a wide range of thermal conditions. They have observed that the cetane number of pure biodiesel is almost 30% higher than that of fossil fuel derived diesel. Due to the higher cetane number, pure biodiesel is more reactive and auto-ignites faster than fossil fuel derived diesel.

S. H. Yoon et al. [4] investigated the combustion and exhaust emission characteristics of ultra-low sulfur diesel (ULSD) and biodiesel on an indirect injection compression ignition engine. The combustion characteristics for diesel and biodiesel have similar combustion pressure and heat release rate behaviors at various engine loads. They have also observed that the ignition delay of biodiesel was slightly shorter than that of ULSD at all conditions because of the high cetane number and oxygen content. The brake thermal efficiency of biodiesel, as well as the hydrocarbon and carbon monoxide emissions of biodiesel, was slightly lower than that of ULSD under low load conditions. However, nitrogen oxides emissions of biodiesel were higher in all engine load conditions.

In Thailand, biodiesel is produced from palm oil via the acid-esterification and transesterification with the methanol process. It is blended with fossil diesel fuel as B7 (7% biodiesel), B10 (10% biodiesel), and B20 (20% biodiesel) for standard commercial form. A. Tripatara et al. [5] investigated biodiesel in Thailand on a single-cylinder diesel engine. They have observed the reduction of heat release rate, owing to the higher cetane number of biodiesel, and the decrease of smoke intensity when the biodiesel mixed ratio increased.

Another alternative fuel which is manufactured from agricultural products such as sugarcane, cassava, and molasses is ethanol. M. Lapuerta et al. [6] investigated modeling the viscosity of butanol and ethanol blended with biodiesel and diesel fuels. They have observed that viscosity values of diesel and biodiesel blends decreases when alcohol content increases. According to C. Zhan et al. [7] and L. Geng et al. [8], low viscosity and density of a given blended fuel was occurred by adding ethanol into biodiesel fuel. It led to better atomization when the fuel was injecting.

Ethanol possesses high oxygen content and a low cetane number [Q. Fang et al. [9] and C. Sayin [10]]. There is an increase of the ignition delay of biodiesel-ethanol blended fuel due to the lower cetane number and higher heat of vaporization of ethanol. The longer premixed duration and higher oxygen content in the blended fuel results in a more complete combustion and the start of the

Table 1
Test engine specifications.

Parameter	Value
Model	Isuzu 4JJ1 TC
Model year	2005
Engine type	Diesel, four stroke
No of cylinder	Four
Bore x Stroke (mm)	95.4 × 104.9
Total displacement (cc)	3000
Injection System	Common rail
Injection Nozzle	Electrical controlled injector
Maximum power output	107kw@3600 rpm
Maximum torque output	294Nm@1400–3400 rpm
Addition devices	EGR, Turbocharger

Table 2
Fuels properties.

Fuel Properties	Standard	B10	B20	B100	Ethanol
Carbon (% mass)	ASTM D 5291	84.66	82.61	76.73	52.2
Hydrogen (% mass)	ASTM D 5291	13.56	13.45	12.45	13.0
Oxygen (% mass)	ASTM D 5291	1.79	3.94	10.82	34.8
Calorific value (MJ/kg)	ASTM D 240	45.63	44.95	39.94	28.05
Viscosity @ 40 °C (mm^2/s)	ASTM D 445	3.0	3.1	4.5	1.2
Density @ 25 °C (kg/m^3)	ASTM D 1298	835	827	875.3	789.0
Distillation (°C)	ASTM D 86-11b				
T10		180	177.4	336.2	77.8
T90		344.2	348.4	352.3	80

combustion process is retarded to the optimum ignition setup point of the unmodified engine. For all the above reasons, adding ethanol into the fuels could minimize the reduction of heat release rate from inappropriate ignition. H. Tse et al. [11] investigated the particulate emissions of diesel-biodiesel-ethanol blends. Adding ethanol could more effectively lower particulate mass and particulate number compared to ULSD.

The major problems of blending diesel fuels with ethanol are poor miscibility and instability of phase separation depending on ambient temperature, duration of mixing, and ethanol percentage [D.C. Rakopoulos et al. [12] and M.M. Jackson et al. [13]]. A. Chotwichien et al. [14] investigated the stability of phase separation by adding palm methyl ester biodiesel (PME) into diesel-ethanol blended fuel. The stability and miscibility of blended fuel could be improved by increasing PME proportion. M. Tongroon et al. [15] has studied the stability of ethanol in diesel-biodiesel-ethanol blends in various ethanol percentages at room temperatures (27–30 °C) and at the lowest winter temperature of Thailand (5 °C). The results showed that higher percentages of ethanol could be added with the increasing biodiesel percentage in the blends.

Plenty of literature about combustion behavior and emission reduction from diesel engine by using biofuel such as methyl ester biodiesel, methanol, and ethanol could be found in recent years. They proved that biodiesel and ethanol have potential to partially replace petroleum diesel to reduce fossil fuel depletion and greenhouse gases emission from petroleum production. Although, there were very few literatures that discussed the impact of different percentages of biodiesel and ethanol in biodiesel, diesel, and ethanol blended fuels. Therefore, the objective of this research is to investigate the effect of difference percentage of biodiesel and ethanol on common rail diesel engine on the viewpoint of combustion and emissions. In this study, all the engine's control systems and test environment were not modified. The fuels chosen for this research are diesel-biodiesel blended fuels (B10, B20, and B100) and diesel-biodiesel-ethanol blends (B10E5, B10E10, B20E5, B20E10, B100E5, and B100E10). The novelty of this research is the testing and analyzing of the effect of renewable biofuels on common rail direct injection diesel engine (without modifying the injection system) by formulating different combinations of the diesel biodiesel-ethanol blends.

2. Methodology

2.1. Engine specification and fuels property

This study was carried out on a commercial 3-L, four-cylinder, diesel engine. The engine's specifications are described in Table 1. The injection system of this engine is the common rail injection system. The injection pressure, injected amount and the timing of the injector opening, and closing are controlled by engine control unit (ECU) based on the acceleration pedal position. The maximum output power is 107 kw, produced at 3600 rpm, and maximum torque of 294 Nm, occurring within the speed range of 1400–3400 rpm. In addition, the engine is mounted with an exhaust gas recirculation (EGR) system to reduce NOx emissions, and turbocharger to enhance the engine power by boosting intake air pressure. Except for the cooling system, the engine systems were not modified for this investigation.

In Thailand, biodiesel is produced from palm fruit and ethanol is produced from sugarcane, cassava, and molasses. The B10 (10 %vol biodiesel and 90 %vol diesel) and B20 (20 %vol biodiesel and 80 %vol diesel) already commercially sold [A. Tripatara et al.] [5].

Table 3
Calorific values of fuels.

Fuels	Calorific Values (MJ/kg)	Fuels	Calorific Values (MJ/kg)	Fuels	Calorific Values (MJ/kg)
B10	45.63	B20	44.95	B100	39.94
B10E5	44.38	B20E5	43.95	B100E5	39.31
B10E10	43.65	B20E10	42.72	B100E10	38.07

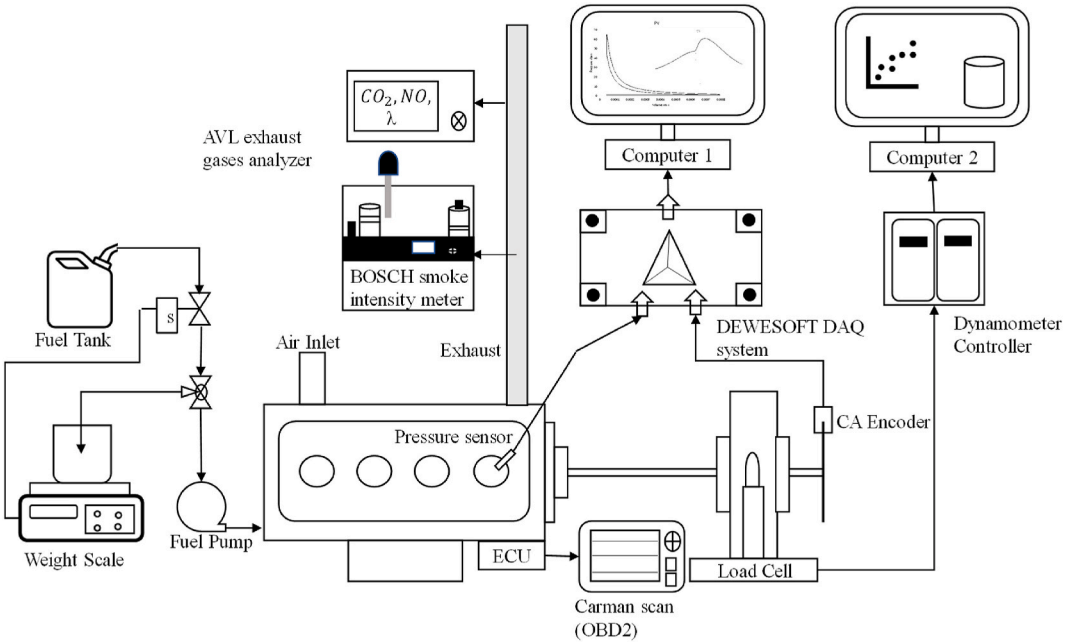

Fig. 1. Schematic diagram of a diesel engine combustion and emission analysis using a water-cooled eddy current dynamometer test bed.

The ethanol used for blended fuels is 99.5% pure ethanol and it is added by 5% and 10% in weight ratio to commercial B10, B20 and B100 fuels. The ethanol blended fuels were named as B10E5 (5%wt ethanol and 95%wt B10), B10E10 (10%wt ethanol and 90%wt B10), B20E5 (5%wt ethanol and 95%wt B20), B20E10 (10%wt ethanol and 90%wt B20), B100E5 (5%wt ethanol and 95%wt B100) and B100E10 (10%wt ethanol and 90%wt B100). The biodiesel from diesel B10 and B20 can serve as emulsifier to keep the mixture as homogeneous solution [P. Kwanchareon et al.] [16]. The properties of base B10, B20, biodiesel and ethanol fuels were mentioned in Table 2. The lower carbon to hydrogen ratio and the higher oxygen content of biodiesel and ethanol may reduce smoke formation because of pyrolysis combustion process [W.G. Wang et al.] [17]. The biodiesel has lower range of distillation temperature but starts boiling at 336.2 °C. The distillation starts at around 180 °C for B10 and B20 fuels while ethanol has the lowest distillation temperatures and lowest range. The low viscosity and density of ethanol will enhance the fuel break-up and atomization of ethanol blended fuels, but ethanol can decrease the fuel lubricity for the injection system. High viscosity biodiesel, on the other hand, will restore the lubricity of the fuel. The calorific values of all tested fuels were tested with Automatic Bomb Calorimeter; Leco model AC – 500 and the results are shown in.

Table 3. As the percentage of biodiesel and ethanol in the fuel increased, the heat of combustion decreased.

2.2. Experimental setup

The schematic diagram of engine and dynamometer test bed is shown in.

Fig. 1. An eddy-current dynamometer, Tokyo Plant model ED-150-LC, was used to apply loads on the engine by coupling it with the dynamometer controller. Constant loads of 56 Nm, 84 Nm, and 140 Nm were applied by dynamometer at an idle low engine speed (1000 rpm), the mid-engine speed (1500 rpm), and the engine speed that produces the maximum torque (2000 rpm). To get the desire engine revolution, the engine is controlled by accelerator pedal. A weight scale was used to measure the fuel consumption. In addition, the ECU was connected to a Carman scan on board diagnosis (OBD) tool, which monitored the engine's conditions such as coolant temperature, oil temperature, throttle position, and EGR position.

The in-cylinder combustion was characterized from the raw data of in-cylinder pressure with crank angle position. A pressure transducer, Kistler 6052C31-piezoelectric crystal, is mounted in the position of glow plug with a designed adapter on cylinder number one. It measures the pressure with the accuracy of ±0.7 bar. A crank angle encoder, CA-RIE-360, was applied to measure the actual-time crank angle position and to calculate the combustion chamber volume. The customized disk with the 720 slits is mounted in-between the sensors gate at the end of dynamometer shaft. The resolution of the encoder sensor is 0.5°. The function is based on

Table 4
Accuracy and uncertainty of measurement devices.

Devices	Accuracy
Eddy current dynamometer (rpm)	±5
Eddy current dynamometer (Load %)	±0.8%
Weight scale (g)	±0.15
Pressure sensor (bar)	±0.5
CA encoder (deg)	±0.2
Thermocouple (°C)	±2.2
Bosch smoke meter (%)	±3%
AVL gas analyzer accuracy	
CO2 (% vol)	±0.3%
O2 (% vol)	±0.02
HC (ppm)	±4
NO (ppm)	±5
λ	0.001

the transmission light principle. An infrared beam is emitted and received at the sensor unit.

For emission, the emission of smoke was measured by BOSCH smoke intensity meter Okuda DSM-240. The soot was collected on the paper filter by using the suction pump mechanism of the smoke intensity meter. The filter paper was measured before and after collecting soot under reflectometer light and indicates the soot content in exhaust gas by percentage. 0% means the clean filter paper, while 100% means the filter paper is black caused by the soot in smoke. Moreover, engine out gases such as carbon dioxide (CO_2), and nitrogen oxide, were measured by AVL exhaust gases analyzer (Model: DITEST GAS 1000). In addition, λ, the air-fuel equivalent ratio, is estimated from the emission result of CO, CO_2, HC and O_2 and generated via AVL exhaust gases analyzer with the accuracy of 0.001. The fuel-air equivalent ratio, φ, is equal to the value of one over λ. The accuracy and uncertainty of all test machines are shown in Table 4. For the better visualization of the quantity of soot trapped on paper filter, images of these filter paper were captured under the scanning electron microscope (SEM).

2.3. Pressure data processing

For combustion characteristics, the data from the pressure sensor and crank angle sensor were stored by a DEWESOFT DAQ system with a total of 1000 cycles when the engine running condition was stable at every set engine condition. Although, the sensor output data in some cycles was unacceptable because of the noise from many interference sources. Therefore, 200 acceptable cycles were filtered out from 1000 cycles and averaged it into one engine cycle. Then, third order least square with seven points method (**Equation** 1) was applied to remove the noise for more accurate results. M.J. Rauckis and W.J. McLean [18] also applied this least square method for raw pressure data smoothing.

$$p_{\theta(\text{smoothed})} = \frac{\{-2\cdot(p_{\theta-3}+p_{\theta+3})+3\cdot(p_{\theta-2}+p_{\theta+2})+6\cdot(p_{\theta-1}+p_{\theta+1})+7\cdot p_{\theta}\}}{21} \tag{1}$$

The compression and expansion pressure versus crank angle data can be used to obtain the quantitative combustion information. The heat release profiles are necessary to discuss combustion phenomena. However, thermal losses account for the difference between gross and net heat release rates. The thermal losses during the mid-load and mid-speed running conditions of turbocharged diesel engines include heat transfer to the cylinder wall, losses from the crevice area, and utilization of heat for fuel vaporization. The detection of these thermal losses will be the extended study of this research. Therefore, heat transfer effects during combustion processes are ignored in the current work and the net heat release rate (NHRR) was calculated based on the in-cylinder pressure data and **Equation** 2 according to J.B. Heywood [19]. The calculation of net heat release rate and cumulative net heat release (CNHR) analysis were performed over the crank angle range of −60°–60° to neglect the heat transfer effects during intake stroke and exhaust stroke.

$$\frac{dQ}{d\theta}\ (NHRR) = \left[\frac{k}{k-1}\right]\cdot P\cdot\frac{dV}{d\theta} + \left[\frac{1}{k-1}\right]\cdot V\cdot\frac{dP}{d\theta} \tag{2}$$

Where:

$\frac{dQ}{d\theta}$ ($NHRR$) = rate of net heat release (J/deg)

k = ratio of specific heat (c_p/c_v), P = pressure (Pa), V = volume (m^3)

$\frac{dV}{d\theta}$ = change of volume with crank angle (m^3/deg)

$\frac{dP}{d\theta}$ = change of pressure with crank angle (Pa/deg)

2.4. Experimental data analysis

In this research, both the indicated and brake parts are discussed on the results and discussion section. The fuel consumption was measured three times per engine conditions by using the weight scale and timer. Losses of work are accounted as the difference between the indicated work and brake work, and included friction losses and pumping losses. The indicated work, which was determined

from the in-cylinder pressure and volume as well as engine speed, was used to calculate the indicated power. On the other side, engine output torque and engine speed were used to compute brake power. Normalizing the mass flow rate of fuel with the respective powers yielded the indicated and brake specified fuel consumption. The input heat energy was calculated from the lower heating value and mass flow rate of fuel. After that, thermal efficiencies were calculated by using Equations (9) and (10).

$$W_{i\ \left(\frac{J}{cycle\cdot cylinder}\right)} = \int_{-360}^{360} P \cdot dV \tag{3}$$

$$\dot{W}_{i\ (kW)} = 4_{(cylinder)} \cdot W_{i\ \left(\frac{J}{cycle\cdot cylinder}\right)} \cdot \frac{N_{(rev.)}}{60_{(s)}} \cdot \frac{1_{(cycle)}}{2_{(rev.)}} \cdot 10^{-3} \tag{4}$$

$$\dot{W}_{b\ (kW)} = 4\pi T_{\left(\frac{N\cdot m}{cycle}\right)} \cdot \frac{N_{(rev.)}}{60_{(s)}} \cdot \frac{1_{(cycle)}}{2_{(rev.)}} \cdot 10^{-3} \tag{5}$$

$$ISFC_{\left(\frac{g}{kW\cdot h}\right)} = \frac{\dot{m}_{f\left(\frac{g}{s}\right)}}{\dot{W}_{i_{(kW)}}} \cdot 3600 \tag{6}$$

$$BSFC_{\left(\frac{g}{kW\cdot h}\right)} = \frac{\dot{m}_{f\left(\frac{g}{s}\right)}}{\dot{W}_{b_{(kW)}}} \cdot 3600 \tag{7}$$

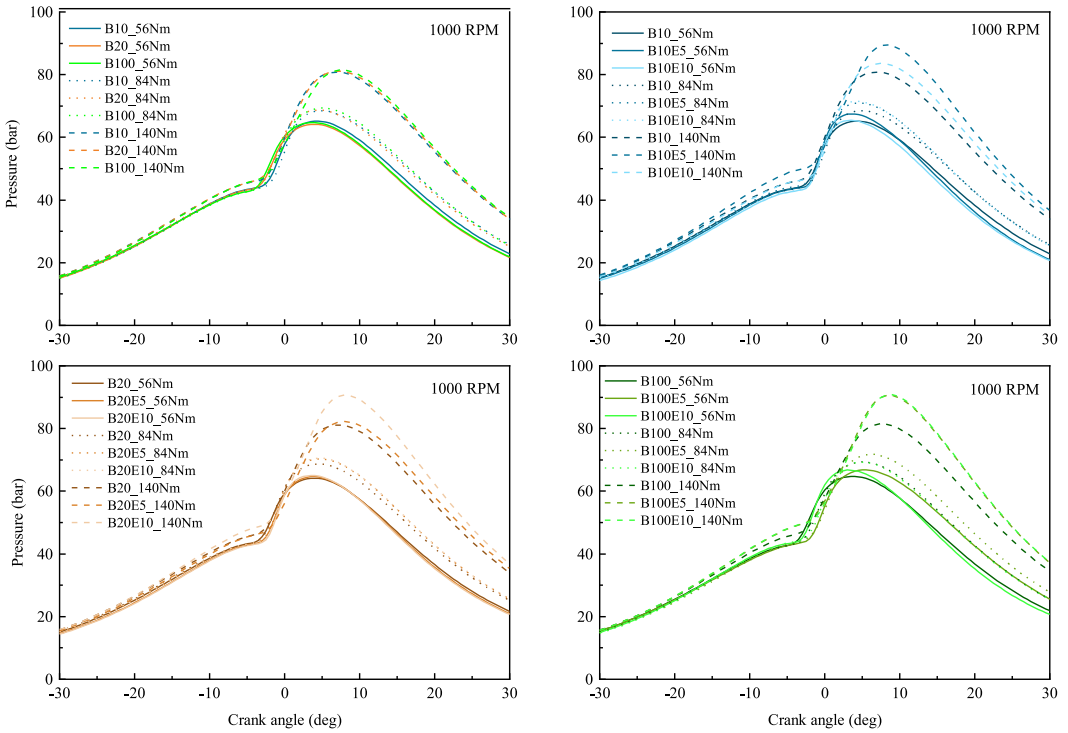

(a)1000 rpm

Fig. 2. Pressure versus crank angle diagrams at (a) 1000 rpm, (b) 1500 rpm and (c) 2000 rpm.

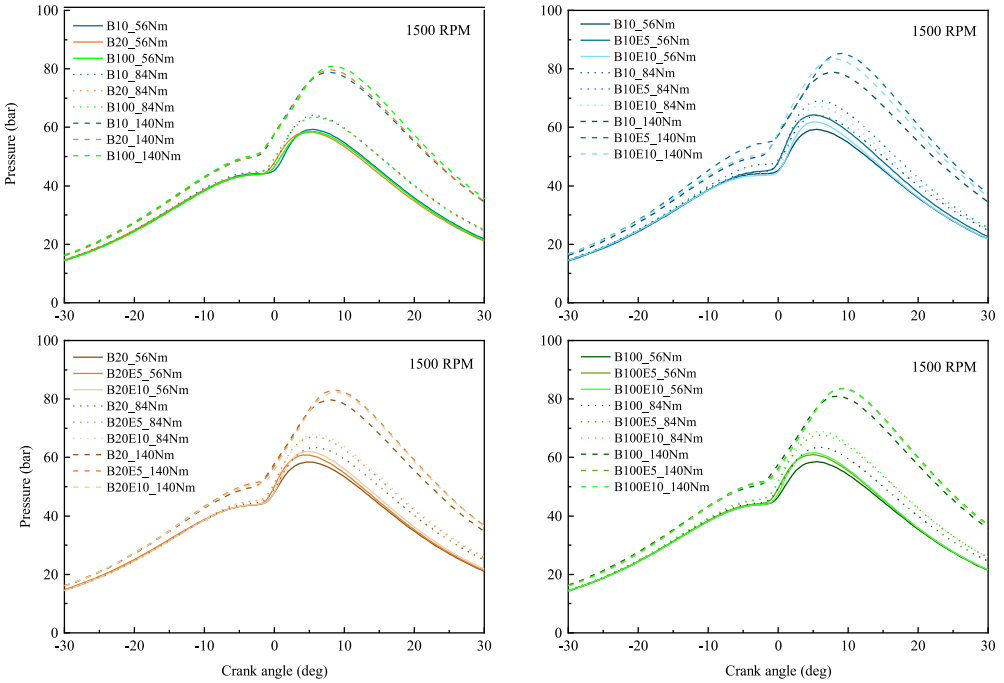

(b) 1500 rpm

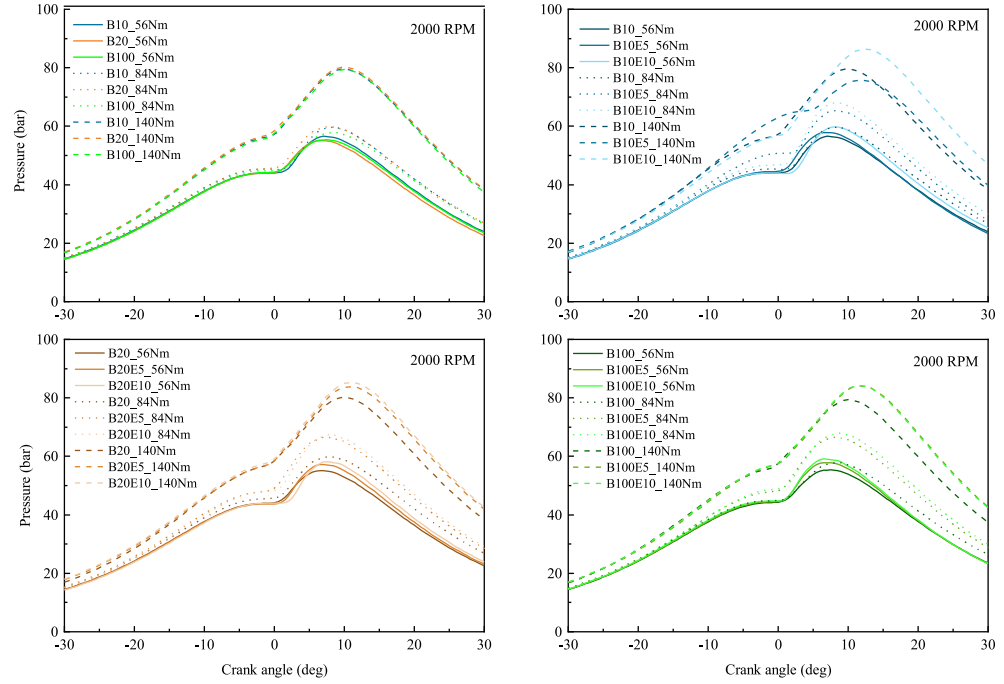

(c) 2000 rpm

Fig. 2. (*continued*).

$$\dot{Q}_{in_{(kW)}} = \underset{\left(\frac{MJ}{kg}\right)}{Q_{LHV}} \cdot \underset{\left(\frac{g}{s}\right)}{\dot{m}_f} \tag{8}$$

$$ITE = \frac{\dot{Q}_{in}}{\dot{W}_i} \tag{9}$$

$$BTE = \frac{\dot{Q}_{in}}{\dot{W}_b} \tag{10}$$

Where, the W_i (J/cycle-cylinder) stands for indicated work for one engine cycle and one cylinder and $\dot{W}_i$ (kW) is the indicated power for all four cylinders. $\dot{W}_b$ (kW) is the brake power. $\dot{m}_f$ is the mass flow rate of fuel in g/s and Q_{LHV} (MJ/kg) is the lower heating value of fuel which neglecting the heating values of hydrogen included in the fuel molecules. In addition, ITE and BTE are the indicated and brake thermal efficiencies.

3. Results and discussion

3.1. Combustion characteristics

The fuels are organized into four groups: (i) B10, B20 and B100 (*top-left graph*), (ii) B10, B10E5 and B10E10 (top-right graph), (iii) B20, B20E5 and B20E10 (botom-left graph), and (iv) B100, B100E5 and B100E10 (*bottom-right graph*). Fig. 2 shows the profiles of pressure versus crank angle of four groups of tested fuels at 1000 rpm, 1500 rpm, and 2000 rpm respectively. The pressure peaks of combustion increases when the engine load increases because more fuel is burnt at higher loads. With regard to engine speed, fuel air mixing duration decreased because of faster combustion cycles at higher engine speeds. Therefore, less fuel are burnt in the premixed combustion phase at higher engine speed than the lower engine speed. As a consequence, the peak pressure is lower with the higher engine speed. Ethanol blended fuels show higher peak of combustion pressure than the fuels without ethanol and it can be seen more obviously in higher engine load conditions. On the other hand, the peak pressure increased with the increasing biodiesel percentage because of fuel oxygen molecules which advanced the combustion efficiency of fuels.

Fig. 3 shows the results of maximum pressure rise rate (MPRR). MPRR is directly proportional to the engine noise and vibration. The maximum pressure increases mainly occurred in the premixed combustion phase. The MPRR of ethanol blended fuels are higher

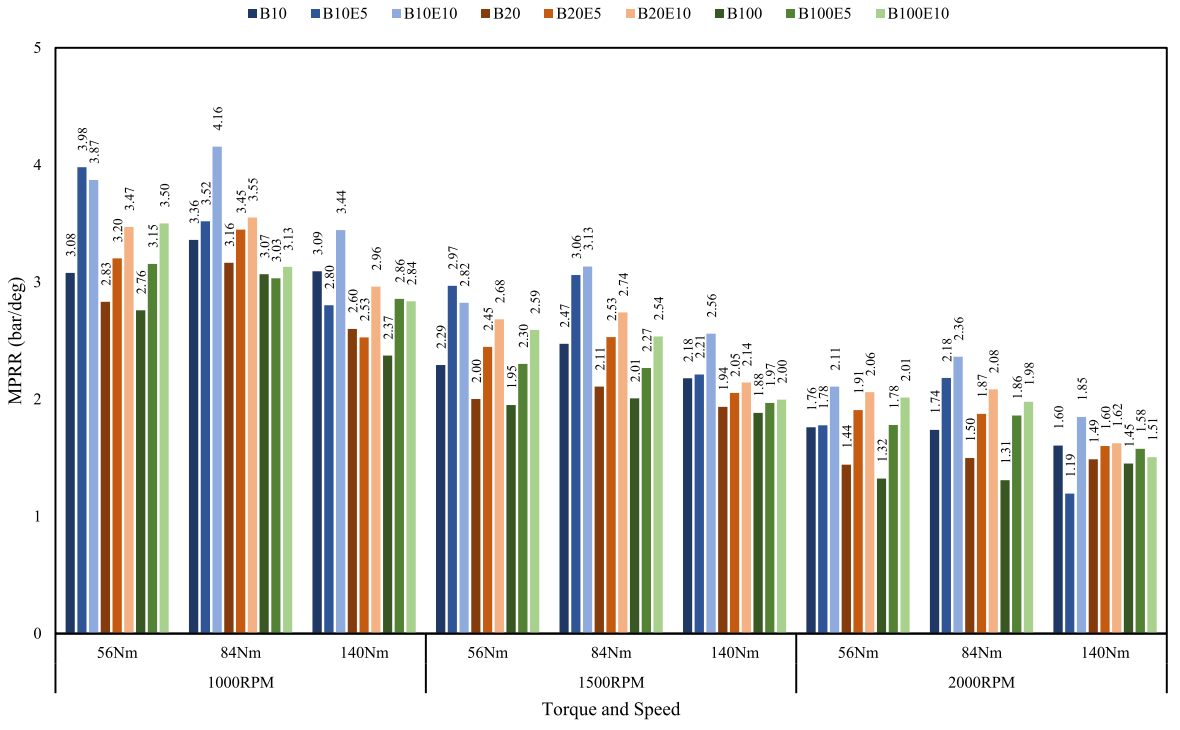

Fig. 3. Comparison of the maximum pressure rise rate in the case of different fuel types, engine speeds and torques.

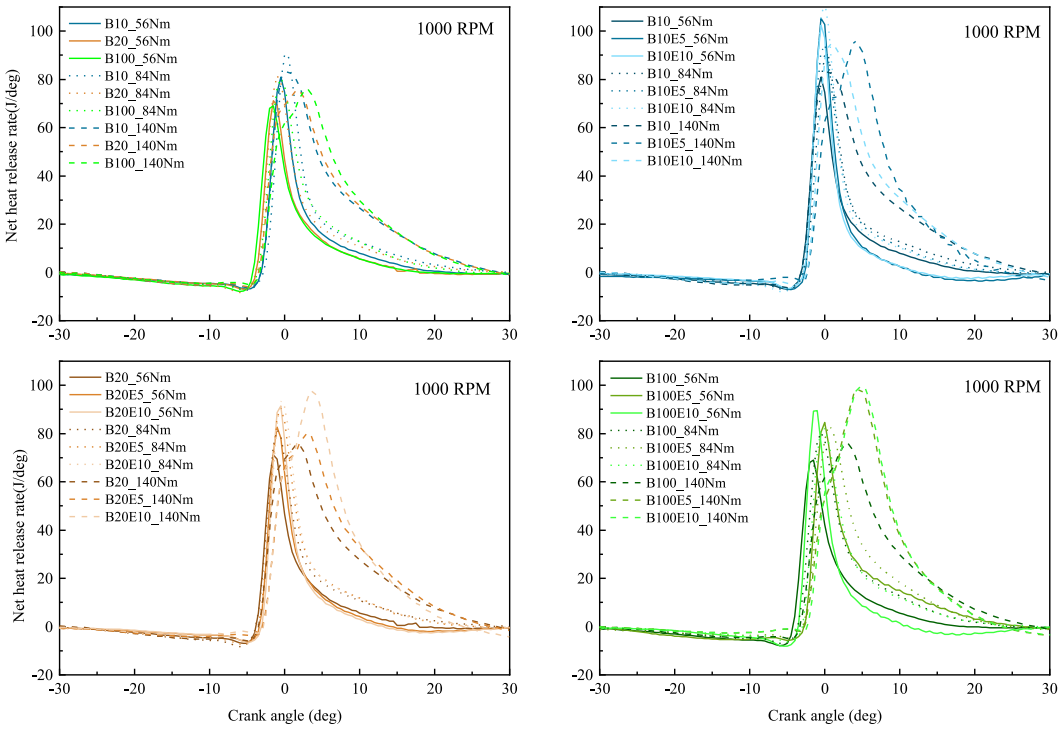

(a) 1000 rpm

Fig. 4. Net heat release rate (NHRR) versus crank angle diagrams at (a) 1000 rpm, (b) 1500 rpm and (c) 2000 rpm.

than that of B10, B20 and B100 based fuels. It increases with the ethanol portion in fuels because the higher atomization properties of lower viscosity and density ethanol blended fuels at the same injection pressure leads to more uniform local air fuel ratio and advances the premixed combustion percentage, and it is similar to the results of H. Huang.et al. [20]. However, when MPRR was examined between that of B10, B20, and B100, it was observed that the MPRR decreased as the biodiesel percentage increased. The MPRR decreases as engine speed increases because there is a drop in the premixed combustion percentage.

All the investigated fuels have the same net heat release rate trends: premixed combustion followed by diffuse combustion. The NHRR graphs are shown in Fig. 4. When the engine speeds are higher, the percentage of premixed combustion phase is narrower because there is less time to mix air and fuel as discussed before. Therefore, the maximum NHRR is found at 84Nm engine load for 1000 rpm and 1500 rpm but at 2000 rpm, it is found at 140Nm engine load. This result agrees with the results of L. Zhu [L. Zhu.et al.] [21]. The cumulative net heat release of all tested fuels is shown in Fig. 5. It is increased with the increasing engine speed and engine load because more fuel was injected to get more power output.

The higher bulk modulus of methyl esters from biodiesel will lead to an earlier start of combustion with the common rail injection system [A.L. Boehman.et al.] [22]. Moreover, injected biodiesel droplets could form low molecular weight compounds inside engine cylinder because of thermal cracking [C.W. Yu.et al.] [23]. These gaseous compounds could ignite easily. As a result, fuels with a higher biodiesel percentage start burning earlier. Because of longer ignition delay among biodiesel fuels, B10 shows the highest peaks of HRR at 56 Nm and 84Nm engine load of every tested engine speeds. At 140Nm engine load, B100 shows the lowest peak of HRR at 1500 rpm and 2000 rpm engine speeds. For the cumulative heat release, B10 is highest at 56 Nm and 140 Nm but B10 is lowest at 140 Nm at every tested engine revolution as well.

The ignition delay time is more prolonged with the increasing ethanol percent because of higher auto ignition temperature, higher heat of vaporization and lower cetane number of ethanol [24]. Because the ignition delay is longer, there is more time for air and fuel to mix, resulting in more fuel combusted in the premixed combustion phase. As a result, ethanol blended fuels provide higher NHRR, in-cylinder pressure, and MPRR. In the diffusion combustion phase, ethanol blended fuels also show higher heat release because the higher fuel oxygen content of ethanol also advanced the combustion during diffuse combustion phase. All the ethanol blended fuels are higher in cumulative heat release than base commercial fuels. This is expected because the oxygen concentration of ethanol blended

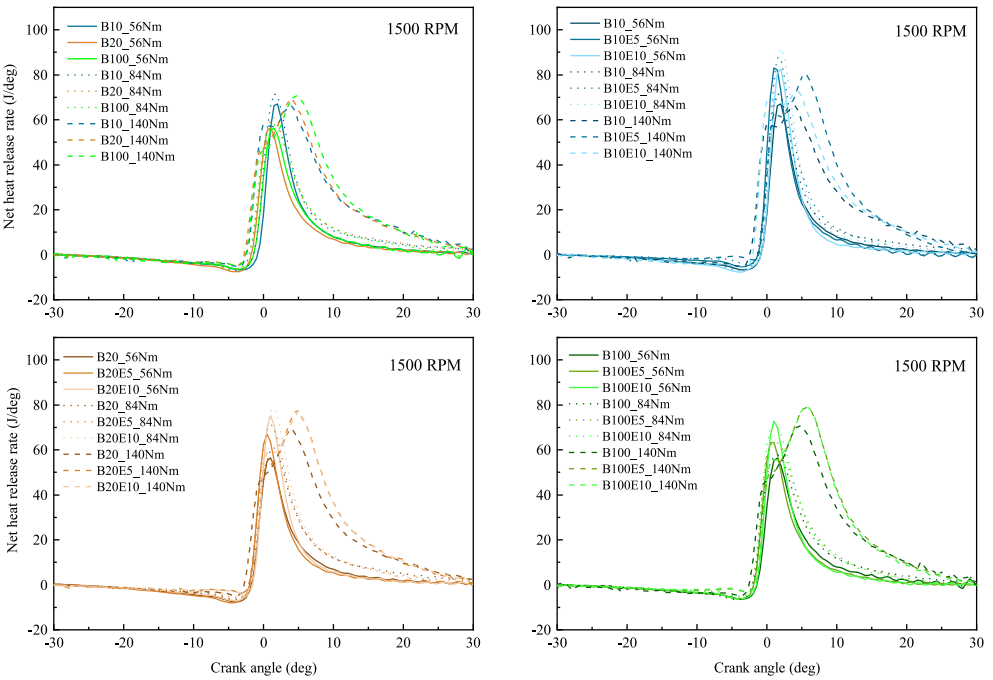

(b) 1500 rpm

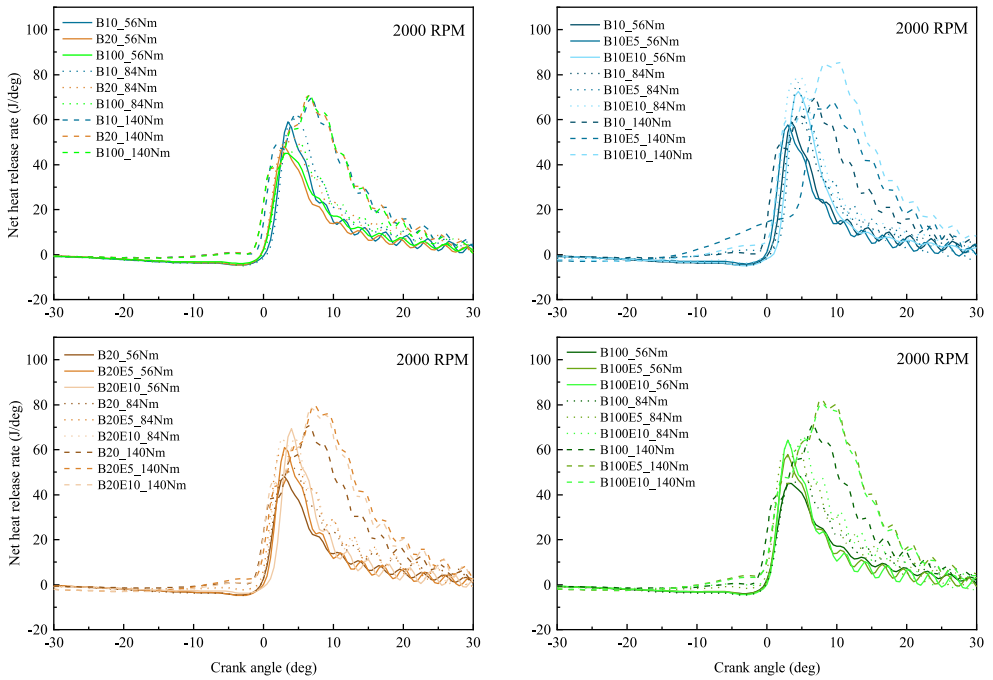

(c) 2000 rpm

Fig. 4. (*continued*).

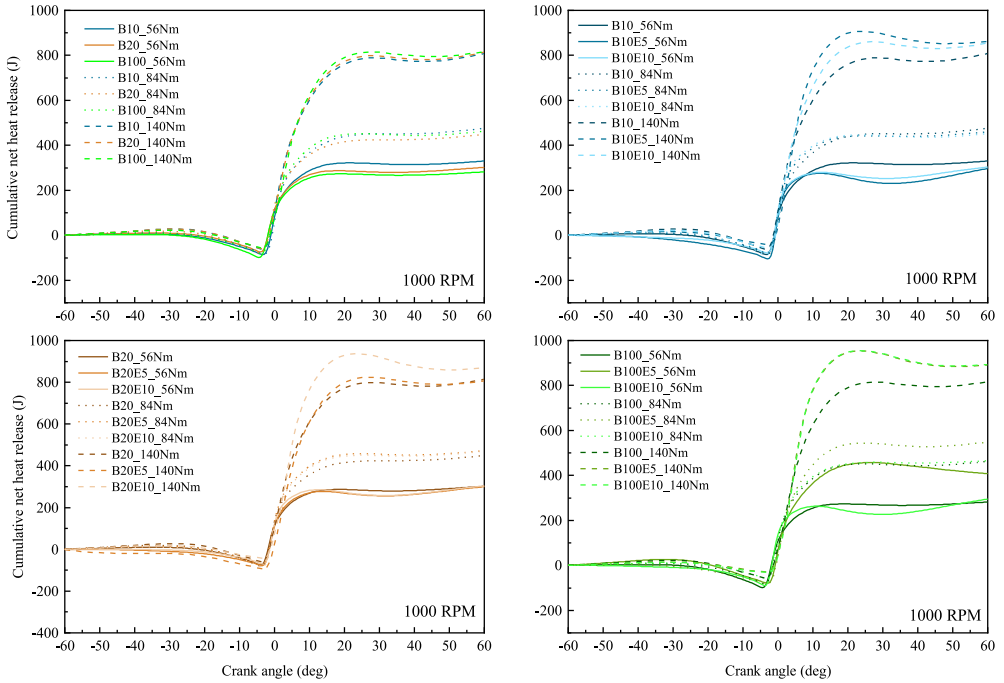

(a) 1000 rpm

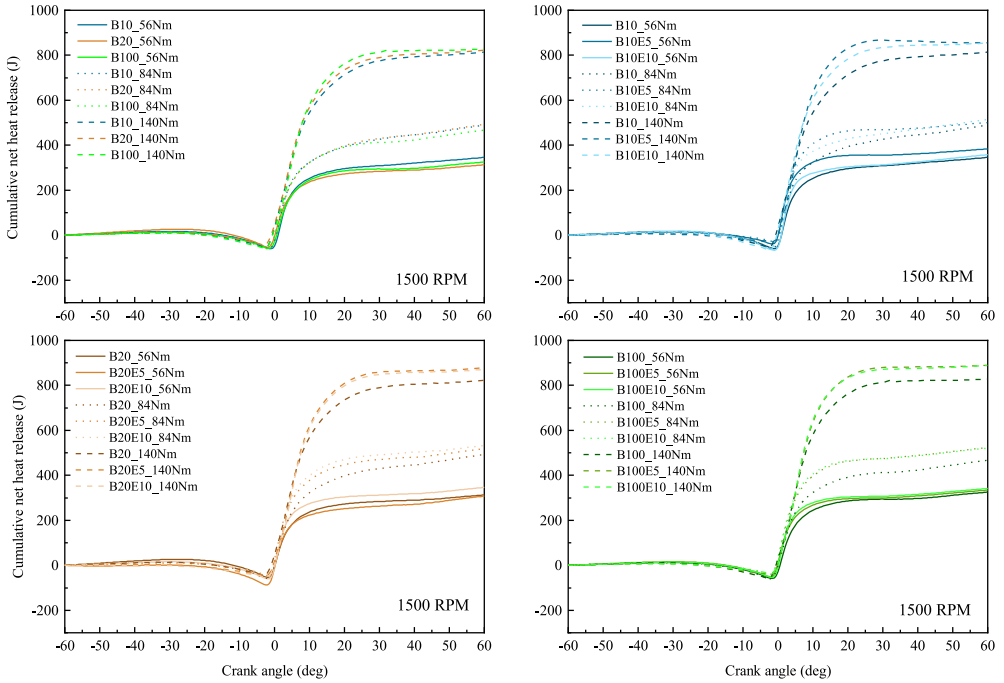

(b) 1500 rpm

Fig. 5. Cumulative net heat release (CNHR) diagrams at (a) 1000 rpm, (b) 1500 rpm and (c) 2000 rpm.

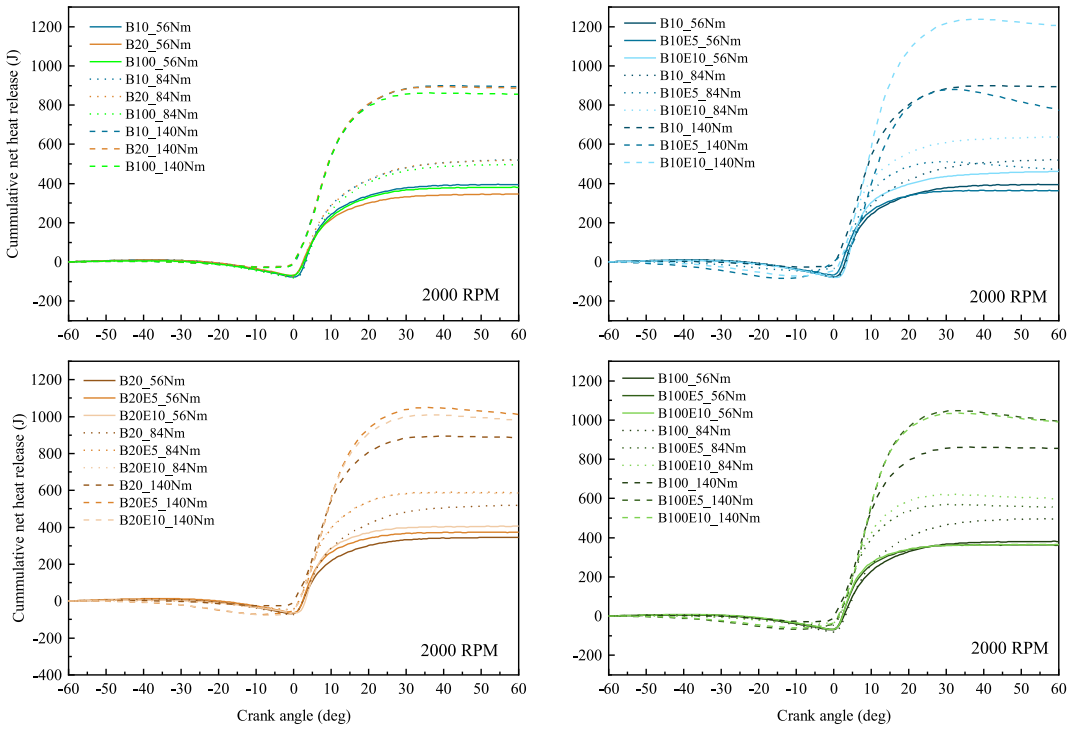

(c) 2000 rpm

Fig. 5. (*continued*).

fuels advanced the combustion quality in both premixed combustion and diffused combustion phases.

Fig. 6 shows the combustion duration of all tested fuels, it is the duration from the start of combustion to the end of combustion. It rises with the increasing engine speed and engine load as more fuel is injected. Higher oxygen content in combustion from intake air or oxygenated fuel diminishes pyrolysis and boosted oxidation, hence resulting the shorter combustion duration [R.J. Donahue and D.E. Foster] [25]. The biodiesel fuel consists of 10.82% mass of oxygen molecules and ethanol consists of 34.8% mass of oxygen molecules. Therefore, the combustion duration is shorter with the increasing biodiesel and ethanol portion in blended fuels.

3.2. Fuel consumption and thermal efficiency

The fuel consumption was measured by weight scale sensor in gram per second and is shown in Fig. 7(a). The brake power, brake specific fuel consumption (BSFC) and brake thermal efficiency (BTE) were calculated from engine speed, torque and fuel consumption. In addition, indicated specific fuel consumption (ISFC) and indicated thermal efficiency (ITE) were estimated from the in-cylinder pressure data and fuel consumptions. Therefore, the difference between indicated factors and brake factors is the friction loss.

When concerning engine load and speed, fuel consumption increases as engine load and speed increases, in order to produce more power output. Because of lower calorific values of biodiesel and ethanol fuels compared to diesel fuel, increasing the proportion of biodiesel and ethanol in blended fuels increases fuel consumption. The ISFC and BSFC are the normalized value of fuel consumption with indicated power and brake power respectively, and mentioned in **Figure** (b,c). Both show the same trends as decreasing with the increasing engine load and speed. However, the ISFC shows lower values than the BSFC, and this contributes to the indicated work being higher than brake work. In comparisons between fuels, the same pattern can be seen in fuel consumption, with a higher BSFC for low energy content fuels. Although, for ISFC, the effect of calorific values among fuels could be observed evidently at low engine speed of 1000 rpm and low engine load of 56 Nm only. The ethanol blended fuels show the lower ISFC than the based fuels becase the better combustion quality of ethanol mixed fuel generate higher indicated power than combustion without ethanol. This feature could be clearly seen in higher engine speeds and engine loads conditions.

Fig. 7(d and e) shows the indicated thermal efficiency and brake thremal efficiency of all tested fuels at all tested modes. When the engine load and speed increased, ITE and BTE continued to increase as well. The rich oxygen content of ethanol could improve the combustion processes and this contributes to the higher thermal efficiency of ethanol blended fuel. The ITE is higher than BTE by

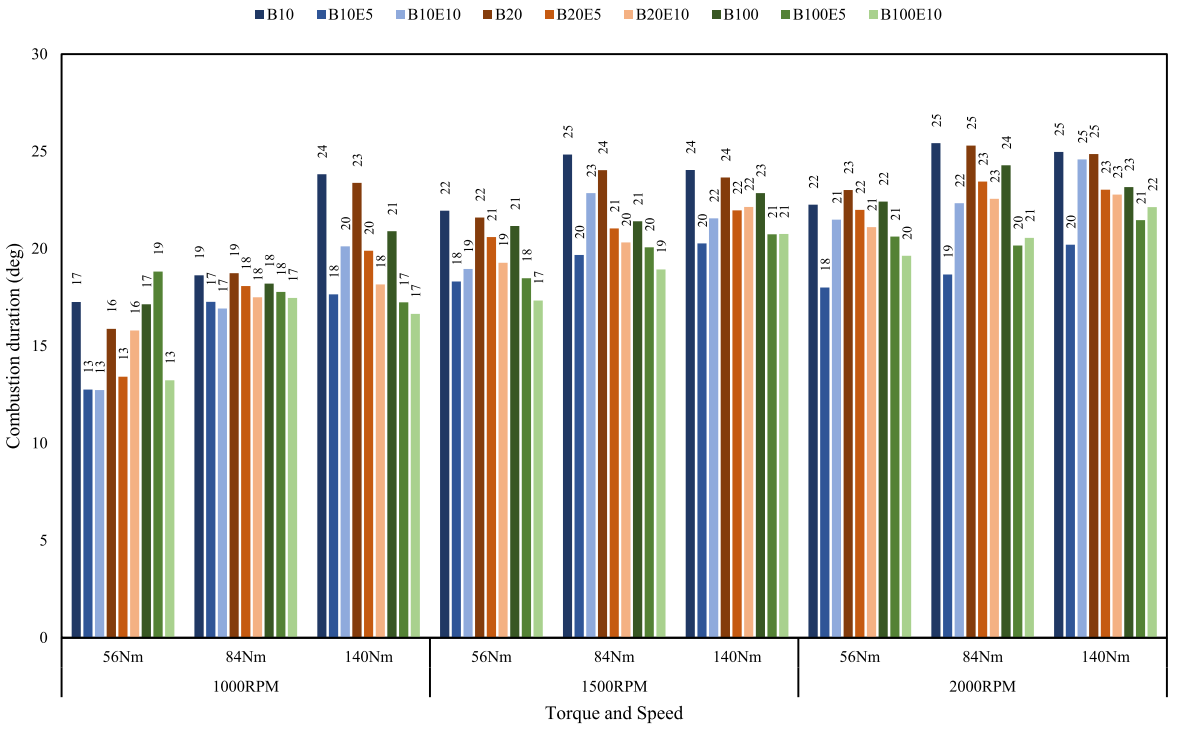

Fig. 6. Comparison of the combustion duration in the case of different fuel types, engine speeds and torques.

around 5 to 10%. In the results of ethanol blended fuels, the wide range of differences were occurred between ITE and BTE. This meant that if an engine was fueled by ethanol blended fuels, the friction losses became higher because adding ethanol degrades the fuel lubricity effect. A wide range of testing parameters was also revealed to be responsible for the variability of results. However, it can be concluded that using the diesel-biodiesel-ethanol blended fuels will not impair the diesel engine's thermal efficiency.

3.3. Emission characteristics

The fuel-air equivalent ratio was automatically estimated back from the emissions of HC, CO, CO2, and O2 and shown in Fig. 8(a). The wider the throttle is opened, the more the volume of intake air is sucked in during the intake stroke. Higher revolutions of the crank shaft led to higher exhaust pressure, resulting in higher boost pressure of the turbocharger. Therefore, equivalent ratio at 1500 rpm and 2000 rpm is lower than equivalent ratio at 1000 rpm which means more air input at 1500 rpm and 2000 rpm. The fuel-to-air ratios increased with the engine loads because more fuel is injected. Because of the increased fuel injection compared to low load situations and lower boost pressure compared to high engine speed, equivalent ratio is highest during 140 Nm - 1000 rpm engine setting for based B10, B20, and B100 fuels. Furthermore, the equivalent ratio is lower with the increasing biodiesel and ethanol content in blended fuels due to oxygen content of biofuels.

Fig. 8(b) depicts the smoke intensity of all the fuels that were tested. It was measured using a smoke intensity meter. The maximum smoke emissions occurred at 140 Nm engine load at 1000 rpm engine speed test mode for B10 and B20 fuels because of heavy load at idle engine speed. The turbo boost pressure at this engine speed is much lower than at 1500 rpm and 2000 rpm leading to less volume of intake air, and thus, 1000 rpm has a higher fuel-to-air equivalent ratio than higher engine speeds. Therefore, this combustion has a richer fuel-air ratio, resulting in more smoke emissions than the other conditions. However, for B100 and other ethanol blended fuels, the smoke emissions do not increase because oxygen content of biofuels could be led to local lean combustion. At idle and medium engine speeds, smoke emissions increase with the increasing engine load because more fuel is injected according to engine loads [Ö. Can.et al.] [26]. While, at 2000 rpm, smoke intensity becomes lower at 140 Nm load than at 84 Nm because of the leaner combustion. When ethanol-biodiesel-diesel mixed fuels were applied, smoke emissions were decreased by almost 75% on average. This is due to the atomic oxygen in ethanol interacting with positive chemical control over the soot generation process [Ö. Can.et al. [26]; Z. Xiao.et al. [27]; PA. Boruff [28]]. During premixed combustion, the local air fuel ratio is very high, hence less soot is formed, but a higher amount of soot formation occurs in the diffuse combustion phase because of fuel-rich combustion [F. Payri.et al.] [29]. As a result, the greater premixed combustion percentage and higher fuel oxygen molecules of ethanol blended fuels lead to decreased soot generation in both the premixed and diffuse combustion phases.

The exhaust temperature was measured by mounting a thermocouple on the exhaust pipe and it is shown in Fig. 8(c). It rises as

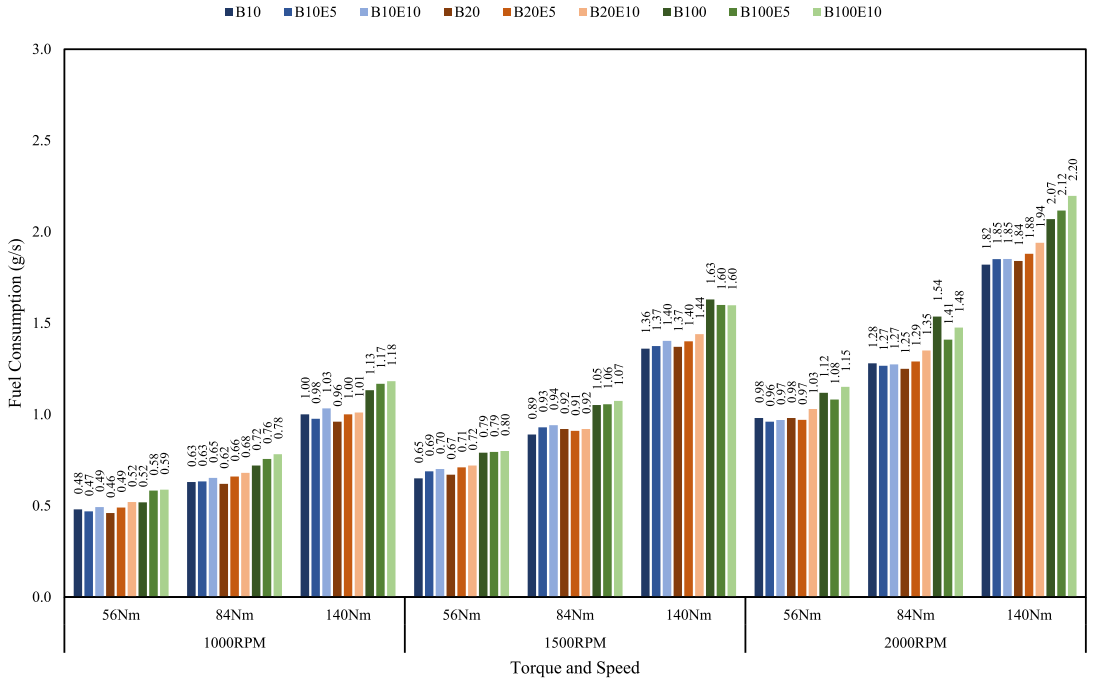

(a) Fuel consumptions

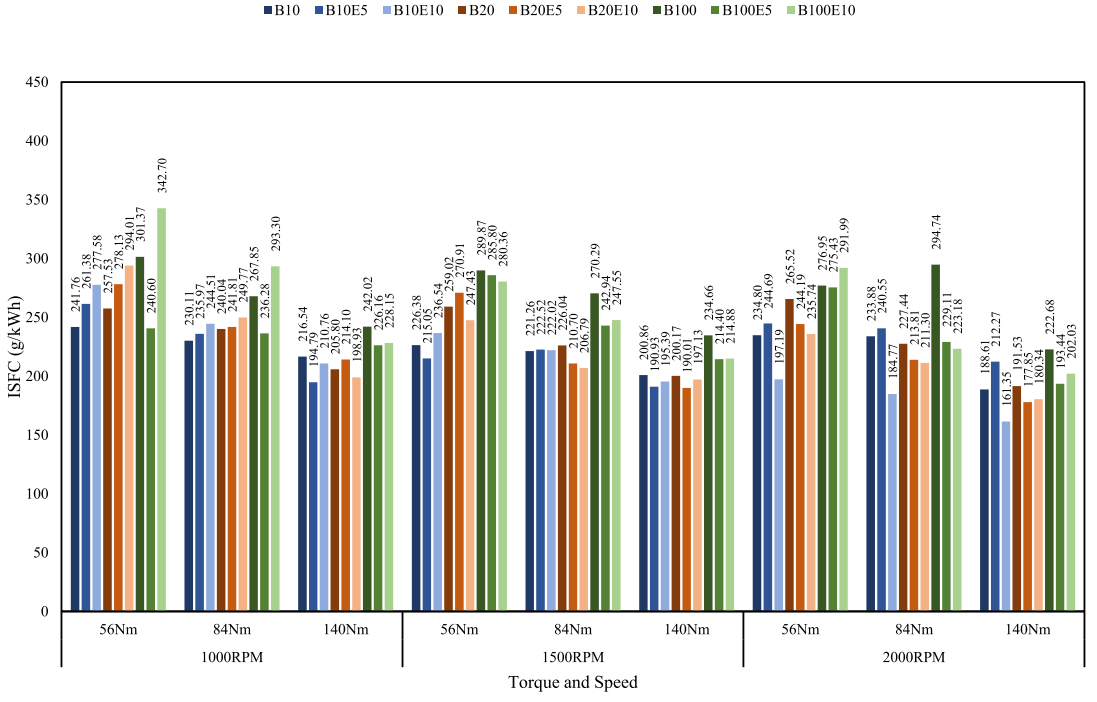

(a) Indicated specific fuel consumptions (ISFC)

Fig. 7. Comparison of (a) Fuel consumption, (b) ISFC, (c) BSFC, (d) ITE and (e) BTE.

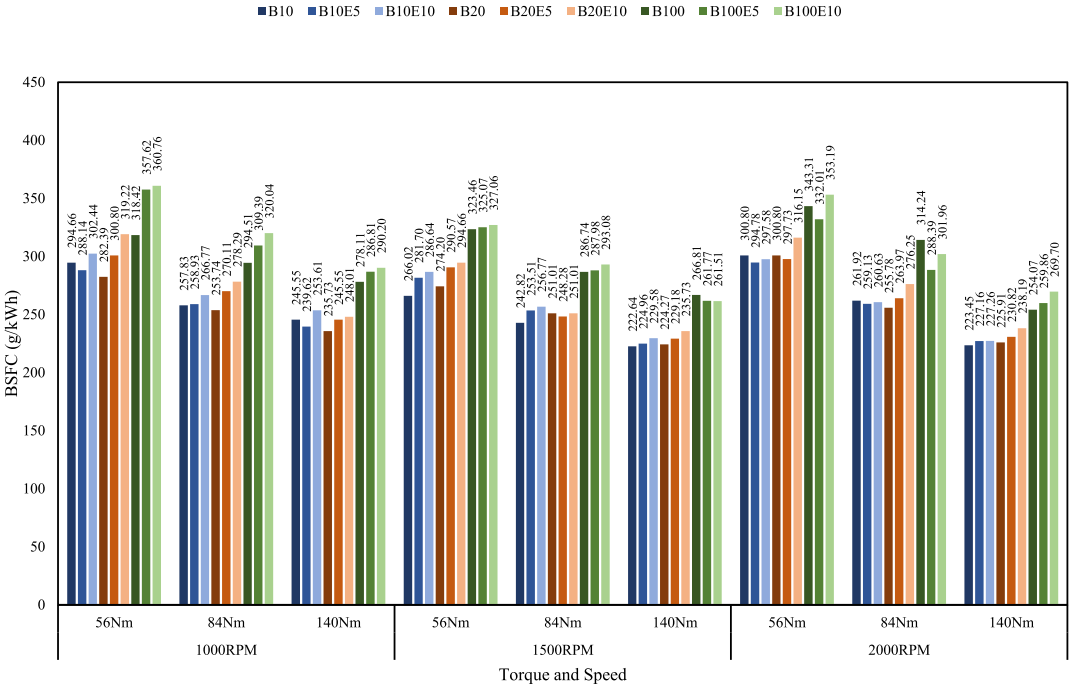

(c) Brake specific fuel consumption (BSFC)

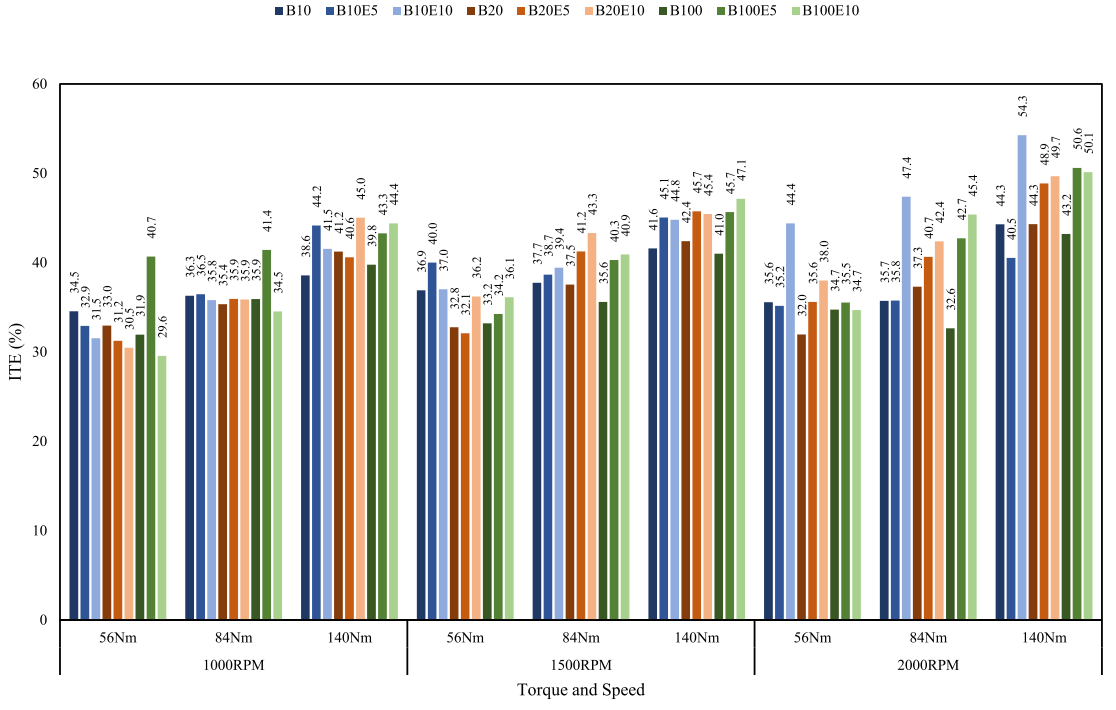

(d) Indicated thermal efficiency

Fig. 7. (*continued*).

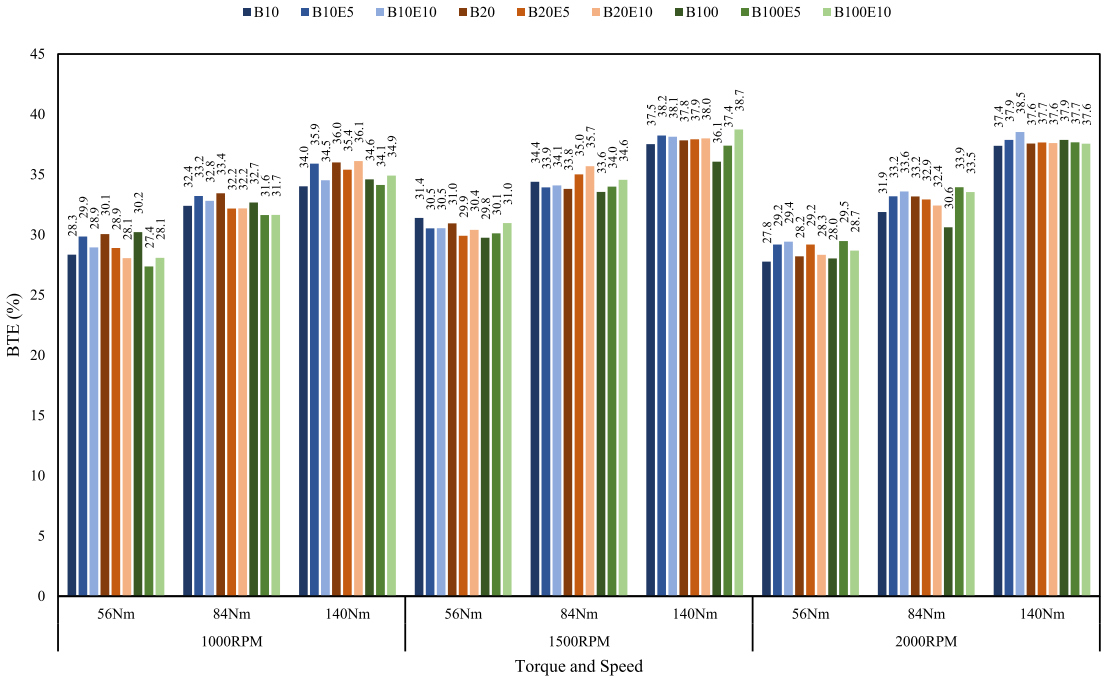

(e) Brake thermal efficiency

Fig. 7. (*continued*).

engine loads and speeds rise since the higher the load, the higher the combustion temperature. The exhaust temperature of ethanol blended fuels is lower than that of biodiesel and biodiesel blended fuels at every engine tested mode. The higher exhaust temperature of commercial base fuels may be the result of the heat emitted during the carbon dioxide formation processes. Fig. 8(d) indicates the amount of carbon dioxide released in percent volume. The fact that base B10, B20, and B100 fuels emit more CO_2 than blended fuels supported the previous discussion point. The lower carbon content of ethanol blended fuel accounts for the reduced CO_2 emissions of ethanol mixed fuels. But the CO_2 emission does not impact the biodiesel content of fuels. It is decreased with the engine speeds because of the leaner combustion but it is increased with the engine loads due to higher fuel injection.

Nitrogen oxide is the most concerning of diesel engine's emissions. The temperature of combustion, oxygen content, reaction time and air fuel equivalent ratio all have a significant impact on NOx emissions [EA. Ajav.et al.] [30]. Fig. 8(e) shows the results of NOx emissions. It is increased with engine speeds and loads because of the higher combustion temperature at high engine speeds and loads. The NOx emissions of all ethanol blended fuels are higher than those of base fuels because of the higher oxygen concentration of fuels and the higher equivalent ratio. The interesting result is found in 140 Nm-1000 rpm engine condition. The results of NOx emissions of B10E10, B20E10, B100E5, and B100E10 are extremely higher, up to over 2000 ppm. That could be expected because the EGR in these conditions was closed to achieve 140 Nm of engine load. Because of their reduced energy level, EGR was closed for these fuels.

The highest smoke intensities were found at 1000 rpm engine speed and 140Nm engine loads condition for all tested fuels. The filter papers, which collected soot at this engine condition, was captured under a scanning electron microscope with 10k magnification and shown in Fig. 9. The morphology of PMs could be observed simply and clearly from the SEM images. The amount of PM decreased with the increasing biodiesel and ethanol percent in blended fuels as B100 is the lowest among B10, B20, and B100. On the other hand, 10% ethanol added fuels emitted the lowest amount of PM between ethanol blended fuels. These observations proved that using oxygenated biofuels may be one of the solutions to reduce PM emissions from CI engines.

4. Conclusions

In this research, ethanol-biodiesel-diesel blended fuels' combustion behavior and emission characteristics were tested on a 3-L, four-cylinder common rail diesel engine with an eddy current dynamometer testbed. The experiment was performed at three engine loads of 56 Nm, 84 Nm, and 140 Nm at the corresponding three engine speed of 1000 rpm, 1500 rpm, and 2000 rpm. The maximum pressure and NHRR is lower with engine speed, but they are higher with engine loads. The cumulative heat release and combustion duration increased as the engine speed and loads increased. The fuel consumption increased with the engine speed and loads while specific fuel consumption decreased. The highest thermal efficiencies were observed at 1500 rpm engine speed.

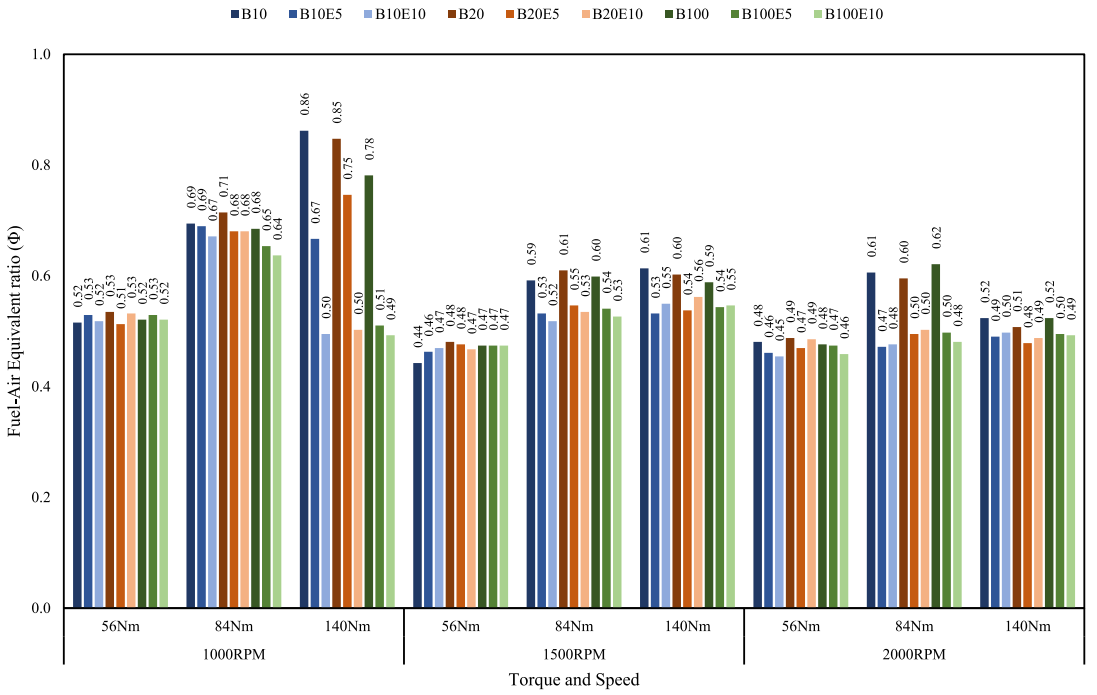

(a) Fuel air equivalent ratio

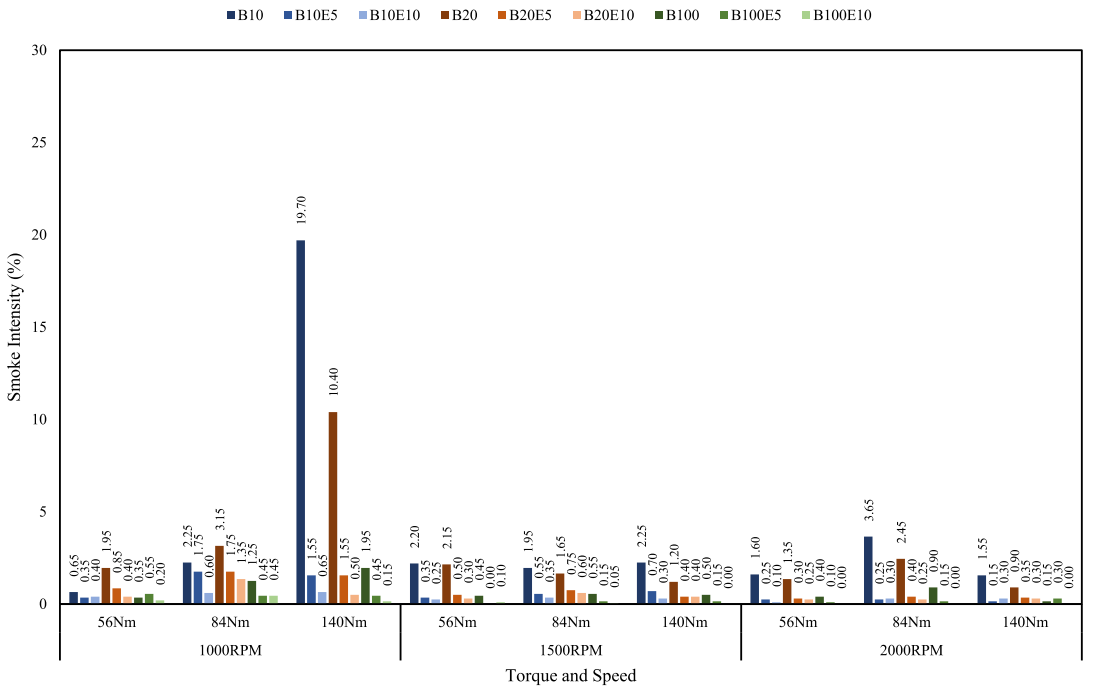

(b) Smoke Intensity

Fig. 8. Comparison of (a) Fuel air equivalent ratio, (b) Smoke intensity, (c) Exhaust temperature, (d) Carbon dioxide and (e) Nitrogen monoxide.

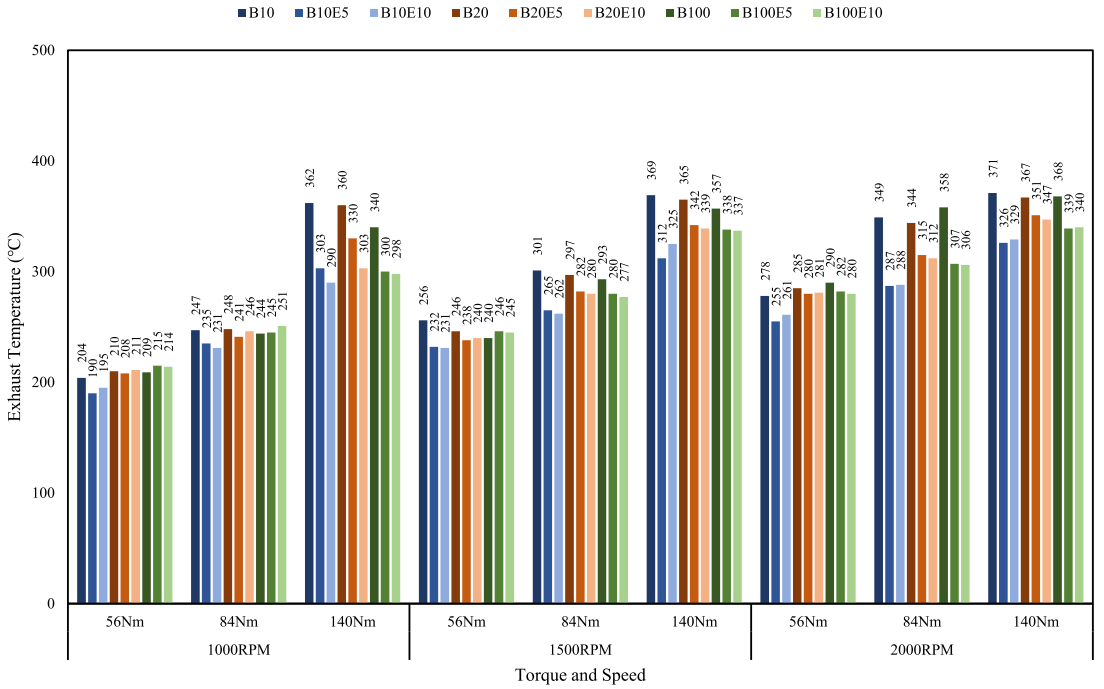

(c) Exhaust temperature

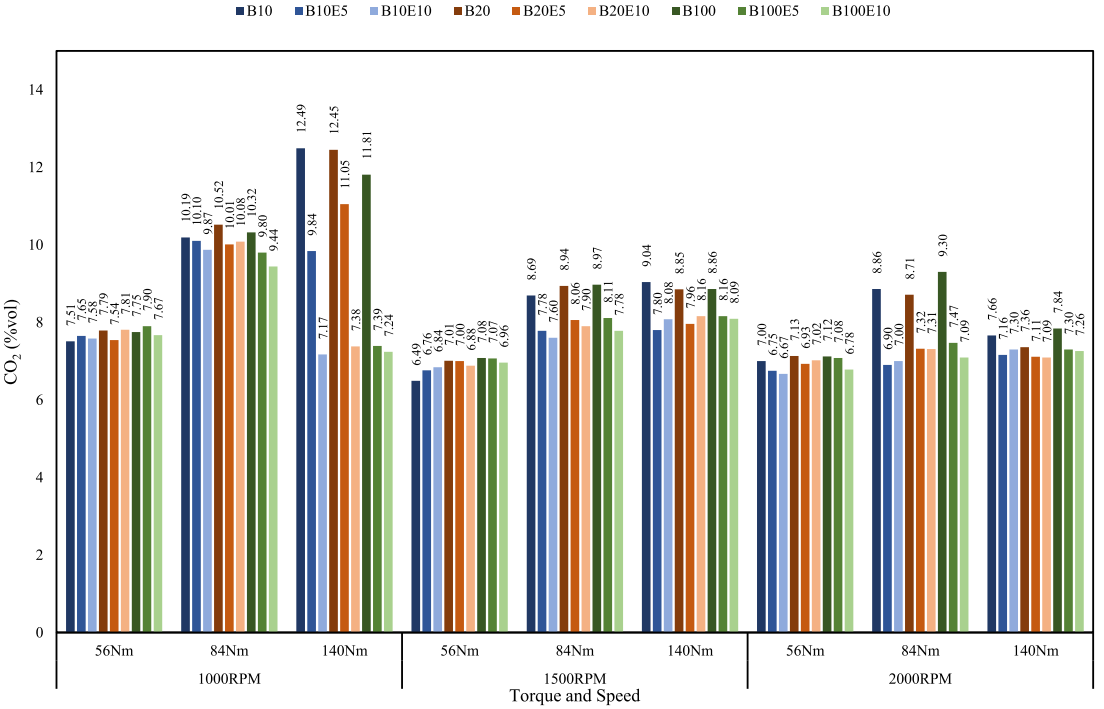

(d) Carbon dioxide

Fig. 8. (*continued*).

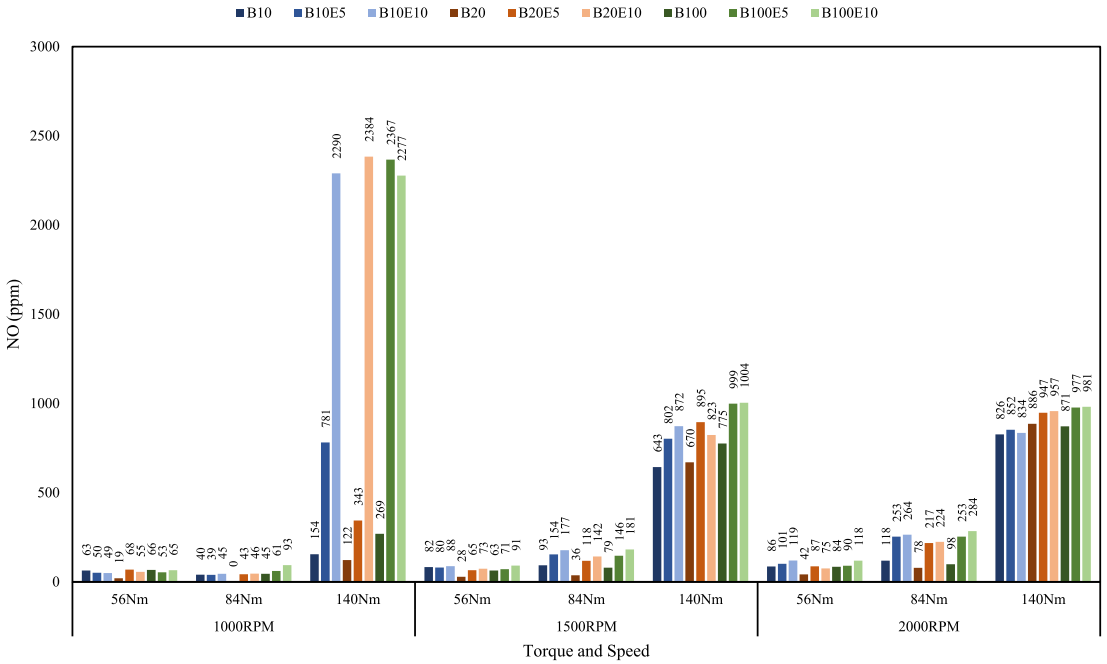

(e) Nitrogen monoxide

Fig. 8. (*continued*).

In comparison between different diesel and biodiesel blende fuels, the combustion starts earlier as the biodiesel percent increased. B10 shows the highest peak pressure, peak of NHRR and highest CNHR at 56 Nm engine load of every engine speed because longer ignition delay time advanced the local air fuel mixing. However, at higher engine load, B100 shows the highest pressure, NHRR and CNHR values. The combustion duration is shorter with the increasing biodiesel content in fuels because the oxygenated fuel speeds up the combustion processes. The fuel consumption increased with the increasing biodiesel percent because of the lower calorific values of biodiesel. Although, it does not significantly impact on engine performance by using biofuels because the energy was recovered from the better combustion of oxygen-rich fuel. The smoke reduction could be clearly observed at 140 Nm – 1000 rpm engine condition. It is decreased by around 50% for B20 and around 90% for B100 than B10 fuel. The formation of nitrogen oxide increased with the biodiesel percent higher while carbon dioxide emissions are similar.

When ethanol is added, because of the higher autoignition temperature, lower cetane number and higher heat of vaporization of ethanol, ethanol-biodiesel-diesel blended fuels need more time for fuel evaporation and led to longer ignition delay. Therefore, higher maximum pressures and maximum NHRRs were observed in every engine condition. The cumulative heat release also increased, and the combustion duration is shorter because there are more oxygen molecules in ethanol mixed fuel. The calorific values are lower and hence fuel consumption is higher for ethanol blended fuels. Thermal efficiency was increased by blending ethanol due to the oxygen content of fuel advanced the combustion processes. Moreover, for emission, the smoke emission decreased by around 50% compared to fuels without ethanol. Nitrogen oxides emissions increased for ethanol blended fuels because of higher combustion temperatures and higher quantity of oxygen molecules.

Author statement

Phyo Wai, Phobkrit Kanokkhanarat, Ban-Seok Oh, Veerayut Wongpattharaworakul: Software, Validation, Formal analysis, Investigation, Resources, Data Curation, Writing - Original Draft Preechar Karin: Corresponding author, Conceptualization, Methodology, Validation, Writing - Review & Editing, Visualization, Funding acquisition, Project administration Nattawoot Depaiwa, Watcharin Po-ngaen, Nuwong Chollacoop, Chadchai Srisurangkul, Hidenori Kosaka, Masaki Yamakita, Chinda Charoenphonphanich: Supervisions.

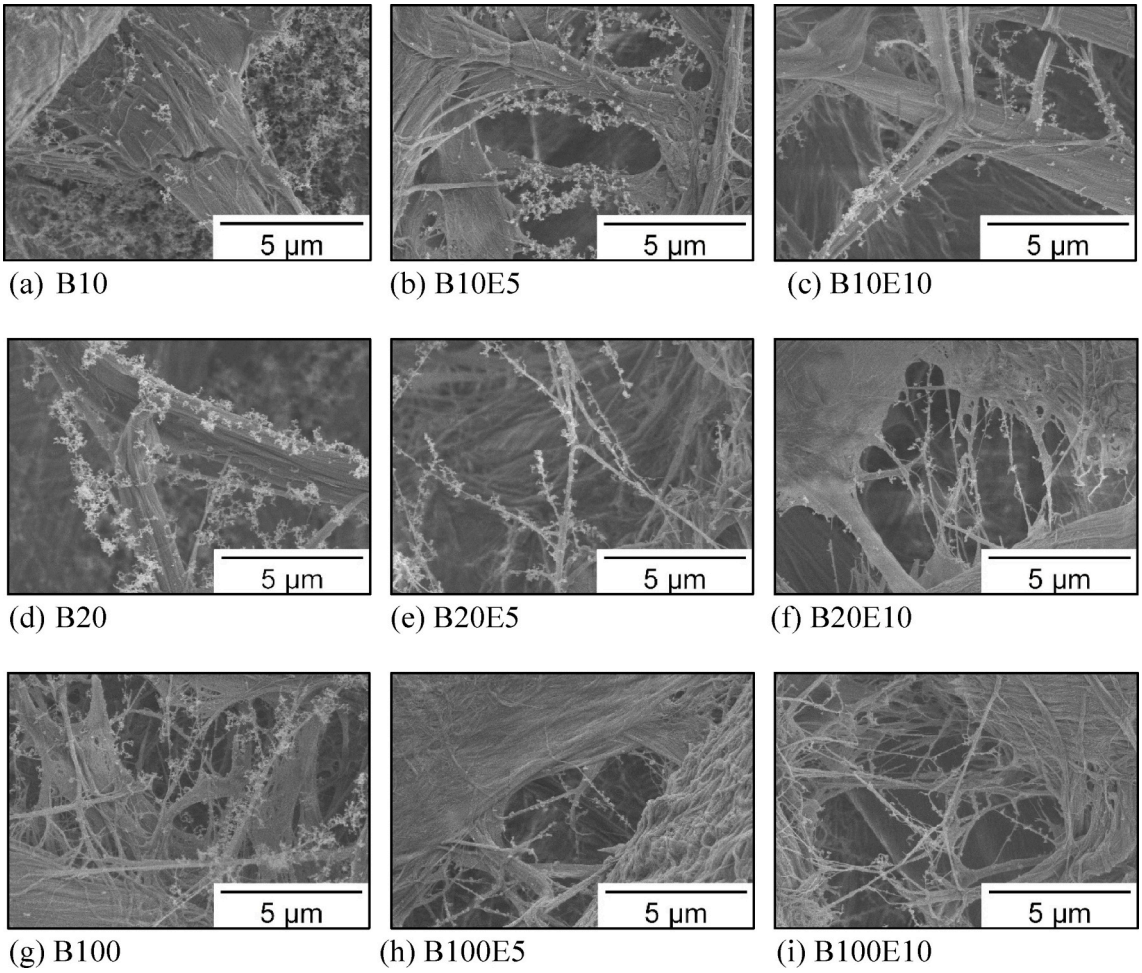

Fig. 9. Comparison of the particulate matters trapped on paper filter in the case of different fuel types, 1000 rpm of engine speed and 140 Nm of engine torque.

Declaration of competing interest

The authors declare that they have no known competing financial interests or personal relationships that could have appeared to influence the work reported in this paper.

Data availability

No data was used for the research described in the article.

Acknowledgements

The authors gratefully acknowledge for research funding from National Research Council of Thailand (Diesel Engine's Particulate Matters Reduction using Ethanol- Biodiesel -Diesel Blends and Particulate Filter 398/2563).

References

[1] R. Zhu, C.S. Cheung, Z. Huang, X. Wang, Regulated and unregulated emissions from a diesel engine fueled with diesel fuel blended with diethyl adipate, Atmos. Environ. 45 (April 2011) 2174–2181.
[2] P. Verma, S. Stevanovic, A. Zare, G. Dwivedi, T.C. Van, M. Davidson, T. Rainey, R.J. Brown, Z.D. Ristovski, An overview of the influence of biodiesel, alcohols, and various oxygenated additives on the particulate matter emissions from diesel engines, Energies 12 (May 2019) 1987.
[3] V.H. Nguyen, M.Q. Duong, K.T. Nguyen, T.V. Pham, P.X. Pham, An extensive analysis of biodiesel blend combustion characteristics under a wide-range of thermal conditions of a cooperative fuel research engine, Sustainability 12 (September 2020) 7666.
[4] S.H. Yoon, C.S. Lee, Experimental investigation on the combustion and exhaust emission characteristics of biogas–biodiesel dual-fuel combustion in a CI engine, Fuel Process. Technol. 92 (May 2011) 992–1000.
[5] A. Tripatara, P. Karin, W. Phairote, C. Charoenphonphanich, M. Masomtob, N. Chollacoop, H. Kosaka, Effect of biodiesel on compression ignition engine's combustion behavior and particle emission, J. Res. Appl. Mech. Eng. (JRAME) 8 (2020) 92–100.

[6] M. Lapuerta, J. Rodríguez-Fernández, D. Fernández-Rodríguez, R. Patiño-Camino, Modeling viscosity of butanol and ethanol blends with diesel and biodiesel fuels, Fuel 199 (July 2017) 332–338.
[7] C. Zhan, Z. Feng, W. Ma, M. Zhang, C. Tang, Z. Huang, Experimental investigation on effect of ethanol and di-ethyl ether addition on the spray characteristics of diesel/biodiesel blends under high injection pressure, Fuel 218 (April 2018) 1–11.
[8] L. Geng, Y. Xie, J. Wang, W. Liu, C. Li, C. Wang, Experimental and numerical analysis of the spray characteristics of biodiesel–ethanol fuel blends, Simulation 97 (August 2019) 703–714.
[9] Q. Fang, J. Fang, J. Zhuang, Z. Huang, Effects of ethanol–diesel–biodiesel blends on combustion and emissions in premixed low temperature combustion, Appl. Therm. Eng. 54 (May 2013) 541–548.
[10] C. Sayin, Engine performance and exhaust gas emissions of methanol and ethanol–diesel blends, Fuel 89 (November 2010) 3410–3415.
[11] H. Tse, C.W. Leung, C.S. Cheung, Investigation on the combustion characteristics and particulate emissions from a diesel engine fueled with diesel-biodiesel-ethanol blends, Energy 83 (April 2015) 343–350.
[12] D.C. Rakopoulos, C.D. Rakopoulos, R.G. Papagiannakis, D.C. Kyritsis, Combustion heat release analysis of ethanol or n-butanol diesel fuel blends in heavy-duty DI diesel engine, Fuel 90 (May 2011) 1855–1867.
[13] M.M. Jackson, K.C. Corkwell, C.C. Degroote, Study of diesel and ethanol blends stability, in: SAE Technical Paper Series, 2003.
[14] A. Chotwichien, A. Luengnaruemitchai, S. Jai-In, Utilization of palm oil alkyl esters as an additive in ethanol–diesel and butanol–diesel blends, Fuel 88 (September 2009) 1618–1624.
[15] M. Tongroon, P. Saisirirat, A. Suebwong, J. Aunchaisri, M. Kananont, N. Chollacoop, Combustion and emission characteristics investigation of diesel-ethanol-biodiesel blended fuels in a compression-ignition engine and benefit analysis, Fuel 255 (November 2019), 115728.
[16] P. Kwanchareon, A. Luengnaruemitchai, S. Jai-In, Solubility of a diesel–biodiesel–ethanol blend, its fuel properties, and its emission characteristics from diesel engine, Fuel 86 (May 2007) 1053–1061.
[17] W.G. Wang, N.N. Clark, D.W. Lyons, R.M. Yang, M. Gautam, R.M. Bata, J.L. Loth, Emissions comparisons from alternative fuel buses and diesel buses with a chassis dynamometer testing facility, Environ. Sci. Technol. 31 (October 1997) 3132–3137.
[18] M.J. Rauckis, W.J. Mclean, The effect of hydrogen addition on ignition delays and flame propagation in spark ignition engines, Combust. Sci. Technol. 19 (April 1979) 207–216.
[19] J. Heywood, Internal Combustion Engine Fundamentals 2E, McGraw Hill Professional, 2018.
[20] H. Huang, W. Teng, Z. Li, Q. Liu, Q. Wang, M. Pan, Improvement of emission characteristics and maximum pressure rise rate of diesel engines fueled with n-butanol/PODE3-4/diesel blends at high injection pressure, Energy Convers. Manag. 152 (November 2017) 45–56.
[21] L. Zhu, C.S. Cheung, W.G. Zhang, Z. Huang, Combustion, performance and emission characteristics of a DI diesel engine fueled with ethanol–biodiesel blends, Fuel 90 (May 2011) 1743–1750.
[22] A.L. Boehman, D. Morris, J. Szybist, E. Esen, The impact of the bulk modulus of diesel fuels on fuel injection timing, Energy Fuels 18 (October 2004) 1877–1882.
[23] C.W. Yu, S. Bari, A. Ameen, A comparison of combustion characteristics of waste cooking oil with diesel as fuel in a direct injection diesel engine, Proc. Inst. Mech. Eng. - Part D J. Automob. Eng. 216 (March 2002) 237–243.
[24] K. Thakkar, S.S. Kachhwaha, P. Kodgire, S. Srinivasan, Combustion investigation of ternary blend mixture of biodiesel/n-butanol/diesel: CI engine performance and emission control, Renew. Sustain. Energy Rev. 137 (March 2021), 110468.
[25] R.J. Donahue, D.E. Foster, Effects of oxygen enhancement on the emissions from a DI diesel via manipulation of fuels and combustion chamber gas composition, in: SAE Technical Paper Series, 2000.
[26] Ö. Can, İ. Çelikten, N. Usta, Effects of ethanol addition on performance and emissions of a turbocharged indirect injection Diesel engine running at different injection pressures, Energy Convers. Manag. 45 (September 2004) 2429–2440.
[27] Z. Xiao, N. Ladommatos, H. Zhao, The effect of aromatic hydrocarbons and oxygenates on diesel engine emissions, Proc. Inst. Mech. Eng. - Part D J. Automob. Eng. 214 (March 2000) 307–332.
[28] P.A. Boruff, A.W. Schwab, C.E. Goering, E.H. Pryde, Evaluation of diesel fuel — ethanol microemulsions, Transactions of the ASAE 25 (1982) 47–53.
[29] F. Payri, J. Benajes, J. Arrègle, J.M. Riesco, Combustion and exhaust emissions in a heavy-duty diesel engine with increased premixed combustion phase by means of injection retarding, Oil Gas Sci. Technol. 61 (March 2006) 247–258.
[30] E.A. Ajav, B. Singh, T.K. Bhattacharya, Performance of a stationary diesel engine using vapourized ethanol as supplementary fuel, Biomass Bioenergy 15 (December 1998) 493–502.